NUMERICAL STUDIES ON AIR RESISTACE REDUCTION METHODS FOR A LARGE CONTAINER SHIP WITH FULLY LOADED DECK-CONTAINERS IN OBLIQUE WINDS

T. V. NGUYEN [1,3,*], N. SHIMIZU [2], A. KINUGAWA [2], Y. TAI [2], AND Y. IKEDA[1]

[1] Research Organization for the 21st Century (RO-21)
Osaka Prefecture University
1-1 Gakuen-cho, Nakaku, Sakai, Osaka 599-8531, Japan
e-mail: dx102001@edu.osakafu-u.ac.jp, web page: http://www.osakafu-u.ac.jp/

[2] Imabari Shipbuilding Co. LTD.
30 Showa-cho, Marugame, Kagawa 763-8511, Japan
e-mail: shimizu.nobuyuki@imazo.com, web page: http://www.imazo.co.jp/

[3] Faculty of Transportation Mechanical Engineering
University of Science and Technology-The University of Danang
No. 54 Nguyen Luong Bang St., Lien Chieu Dist., Danang, Vietnam
email: nvtrieu@dut.udn.vn, web page: http://www.dut.udn.vn/

Key words: Numerical Method, CFD, Air Resistance, Container Ship

Abstract. In this study, the aerodynamic characteristics of the complex air flows acting on a large container ship model are numerically investigated by using a commercial CFD code. The main target is to reduce the air resistance in oblique winds, especially at the small angle of wind directions. Some container side-covers with different size and location are developed to shut the gap flow, and a center wall is also applied. The numerical results show that the air resistance at 30degrees of wind direction can be reduced significantly up to 50%, 30% and 15% by full side-covers, front-half side-covers and lower front-half side-cover, respectively.

1 INTRODUCTION

Now a day, the newly designed container ships become very large and the number of containers on deck has increased rapidly. Consequently, the air resistance acting on the ship also becomes larger and the maximum value usually occurs at 20-40degrees of wind direction conditions. Therefore, reducing the air resistance of such ships in oblique winds must be paid attention in order to reduce the fuel consumption and CO_2 emission from the international shipping.

Ouchi [1] studied on air resistance reduction of a large container ship in the sea. Their study showed that covering all longitudinal gaps among container blocks has a great effect on decreasing the longitudinal resistance around 60 degrees of wind direction.

Kim [2] studied on superstructure modification for air resistance reduction of a large container ship. Gap-protector between containers stacks and a visor in front of the upper deck are found to be the most effective ways for air resistances reduction in wide range of heading

angle of winds.

Recently, Watanabe [3] & Nguyen [4] numerically and experimentally studied on the air resistances reduction methods for a 20,000TEU container ship model with full containers on deck. They developed different types of apparatuses, which can reduce the air resistance.

In this study, the aerodynamic characteristics of the complex air flows acting on the same large container ship model as that using in their studies are numerically investigated by using a commercial CFD code. The main target is reducing the air resistance in oblique winds, especially at the small angle of wind directions. Effects of a full and some partial side-covers with different size and location as well as a center-wall to shut the gap flow are numerically examined.

2 PRINCIPAL PARTICULARS OF SHIP AND MODEL

The main particulars of the 20000TEU container ship and its scale model are presented in Table 1.

Table 1: Principal particulars of ship and model

	Unit	Ship	Model
Scale		-	1/255.3
L_{OA}	m	400	1.560
L_{PP}	m	383	1.50
Breadth (B)	m	58.5	0.230
H	m	49.02	0.192
draft	m	14.5	0.0570
A_F	m^2	2890	0.0443
A_S	m^2	18000	0.2762

The side profile and frontal shape of the ship model can be seen in Fig. 1.

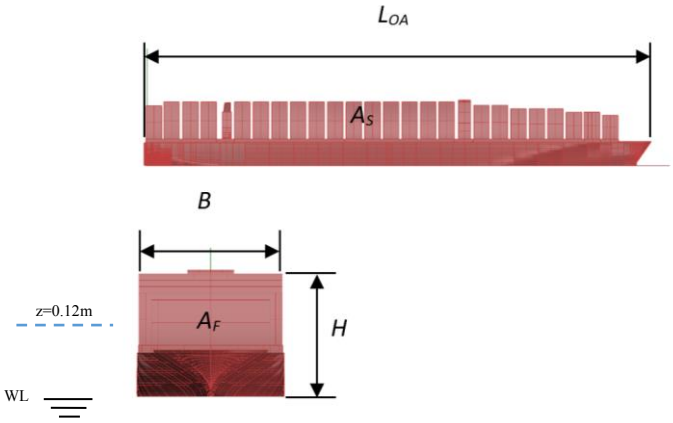

Figure 1: Ship model (Full loaded condition)

3 AIR RESISTANCE REDUCTION METHODS

In previous studies [1]–[4] it has been already confirmed that the gaps between container

blocks on deck increase the air resistance acting on container ships. It was reported that covering the all gaps by using the full side covers [1] or gap protectors [2] can significantly reduce the air resistance. However, in practical, the very large and heavy side-covers increase the ship's weight. In this study, the effects of two kinds of partial side-covers with lighter weight on the reduction of air resistance are numerically examined. In the previous studies of the authors, the gap flows of the front part of the ship considerably generate the wake and increase the air resistance in head winds [4]. Therefore, partial covers at the front part of deck containers can be effective even in oblique winds.

Another alternative is a center wall, which may be, shut the horizontal gap flow at the middle of each gap.

The ship models with the full side-covers, the front side-covers, the front-half side-covers and the center wall can be seen in Figs. 2~5.

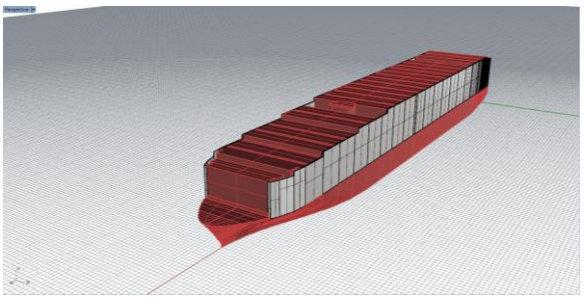

Figure 2: Full side-cover

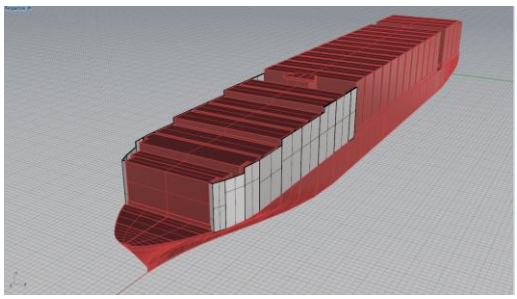

Figure 3: Front side-cover

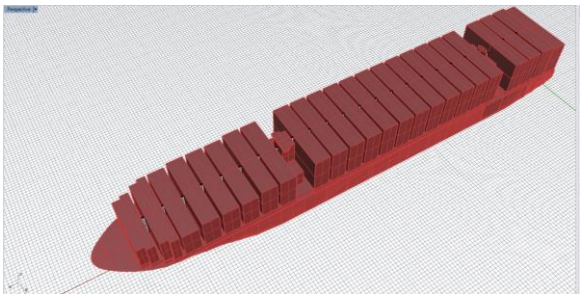

Figure 4: Center wall

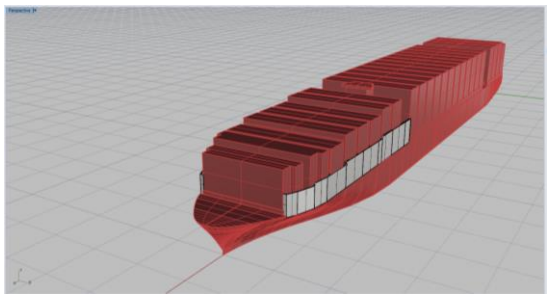

Figure 5: Front-half side-cover

4 COMPUTATIONAL FLUID DYNAMICS

A CFD commercial code, ANSYS Fluent V14.5 is used to solve the RANS equations. The computational domain, coordinate system, mesh generation, and numerical setup are discussed in the following sections. The calculated results were evaluated by comparing the results with experimental results of the ship without and with full side-covers [3].

4.1 Computational Domain

The computational domain is determined as shown in Fig. 6 according to check the

accuracy with the experimental results [3].

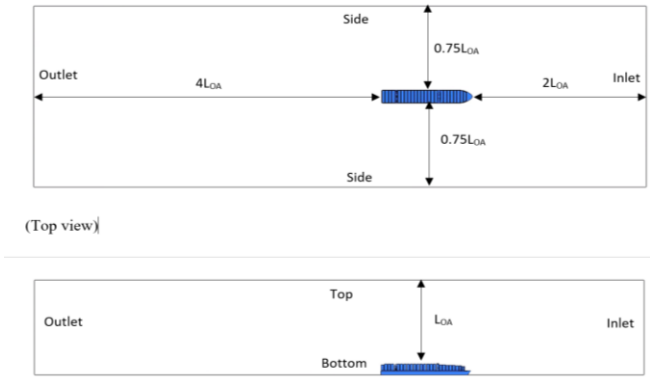

Figure 6: Computational domain

4.2 Coordinate System and Coefficients

This study uses the same coordinate system as the experimental measurement, which has been carried out by Watanabe [3]. The coordinate is shown in Fig. 7.

The aerodynamic coefficients, C_X, C_Y, and C_N are defined as Equations 1~3.

$$C_X = X_A / (\frac{1}{2}\rho_A U^2 A_F) \tag{1}$$

$$C_Y = Y_A / (\frac{1}{2}\rho_A U^2 A_S) \tag{2}$$

$$C_N = N_A / (\frac{1}{2}\rho_A U^2 A_S L_{OA}) \tag{3}$$

Where: C_X, C_Y, C_N are a longitudinal force (air resistance), side force, yaw moment coefficients, respectively, ρ_A is air density (kg/m^3), and U is velocity at the free stream (m/s).

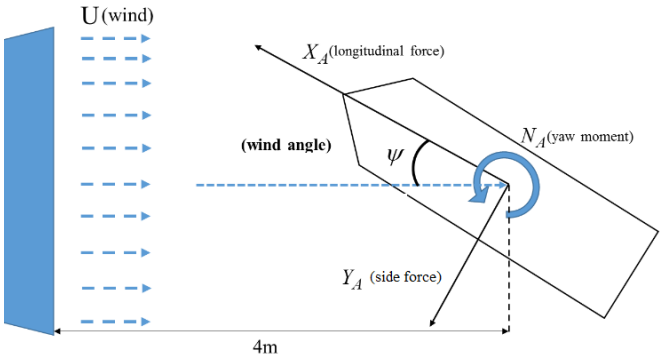

Figure 7: Definition of coordinates [3]

4.3 Mesh Generation

The computational domain is discretized into the mesh cells. Meshing is an important step because of the mesh quality significantly effects on the numerical results. In this study, due to the complexity of the model, the unstructured mesh is generated in ANSYS Meshing module rather than try to obtain the structured mesh. The total number of the mesh is approximate 4.6 million tetrahedral cells. The maximum skewness is less than 0.9. The dimensionless value of the first mesh, y+, is less than 180 for the k-epsilon model. The cut mesh near the model surfaces is shown in Fig. 8.

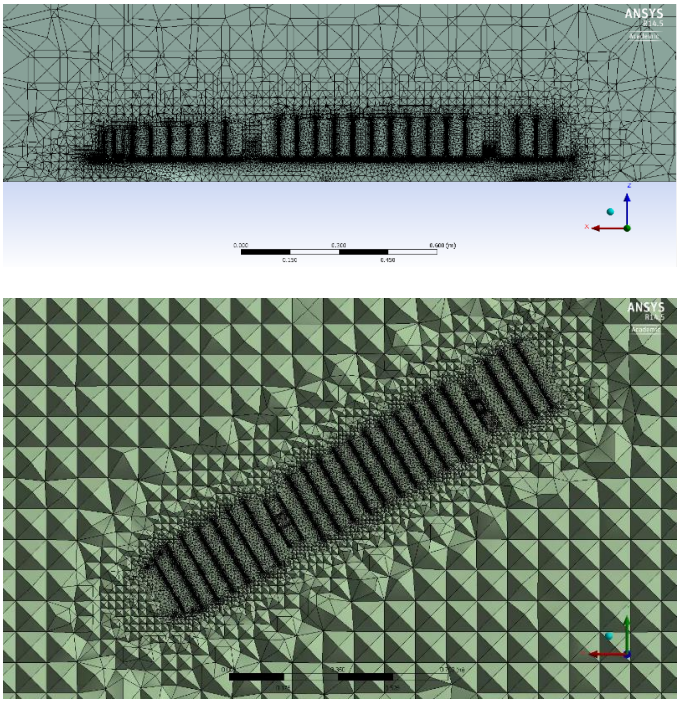

Figure 8: Cut mesh near the surfaces at y=0 (upper), and z=0.12m (lower)

4.4 Solution Setup

The k-epsilon turbulence model is used. The standard wall function is applied for near wall treatment. The velocity inlet and pressure outlet are applied for inlet and outlet boundaries, respectively. A no-slip wall condition is applied to the ship model surfaces, and slip conditions are applied to the top, bottom, and sides of the domain. The second order upwind is selected for the momentum, turbulent kinetic energy, and turbulent dissipation rate to increase the solve accuracy.

The aerodynamic coefficients can be regarded to be independent of the wind speed and free stream turbulence intensity [2]. Therefore, the inflow speed is fixed at 10 m/s, and 5% is selected for the turbulent intensity.

All the setup parameters are listed in Table 2.

Table 2: Solution setup for CFD

Solver	
Type	Pressure-Based
Velocity formulation	Absolute
Time	Steady
Models	
Viscous model	k-epsilon (2 eqs)
k-epsilon Model	Standard
Near-Wall Treatment	Standard Wall Function
Materials	
Fluid	Air
Density	1.225 (kg/m3)
Viscosity	1.7894e-05
Boundary Conditions	
Inlet	Velocity inlet: Velocity Magnitude: 10 (m/s) Turbulent Intensity: 5% Turbulent Viscosity Ratio: 10
Outlet	Pressure outlet: Backflow Turbulent Intensity: 5% Backflow Turbulent Viscosity Ratio: 10
Ship	No-slip wall
Top, bottom, sides	Slip wall
Solution Methods	
Pressure-Velocity Coupling	
Scheme	SIMPLE
Spatial Discretization	
Gradient	Least Square Cell Based
Pressure	Standard
Momentum	Second Order Upwind
Turbulent Kinetic Energy	Second Order Upwind
Turbulent Dissipation Rate	Second Order Upwind

5 RESULTS AND DISCUSSIONS

In the previous papers [3] [4], the aerodynamic forces calculated by the CFD code in the same manner as in the present paper were compared with the experimental ones and showed a fairly good agreement with the experimental ones in all wind directions. Therefore, the accuracy of the CFD simulation was evaluated.

On the basis of the CFD results, the effects of the full side-covers on the velocity and pressure distribution, velocity vector and streamline again are discussed, and the effects will be compared with those of the front side-covers, the front-half side-covers, and the center-wall.

5.1 Velocity and Pressure

The velocity and pressure distribution on the horizontal plane at z=0.12m are shown in Figs. 9-11. The z denotes the distance between the plane and the water surface, and the plane is located at near middle height of the deck containers as shown in Fig. 1.

The velocity and pressure distributions around the deck containers of the ship model without covers are shown in Fig. 9. The velocity distribution shows that very low velocity regions are created at the bow starboard region as well as behind the rear container blocks. The pressure distribution shows that high pressure acts on each corner of the containers. The pressure causes the air resistance increase by gap flows.

The velocity distributions around the deck containers with the three kinds of side-covers and the center-wall wake shown in Fig. 11 demonstrate that the flows around the containers are changed by the covers and the wall. The full side-cover and the front side-cover make a high flow at the front corners in starboard side, and the low velocity regions behind the front container blocks disappear. This may be caused by shutting the gap flows. The velocity distributions of the center-wall and the front-half side-covers are similar to that of the model in standard full-loaded condition.

The pressure distributions are shown in Fig. 11 show that high pressure acting on each corner of the deck containers disappears for the full side-covers and the front side-covers. For the case of the center wall, the high pressures at each corner of the gap entrance act as the same as the case of the conventional deck containers without any covers.

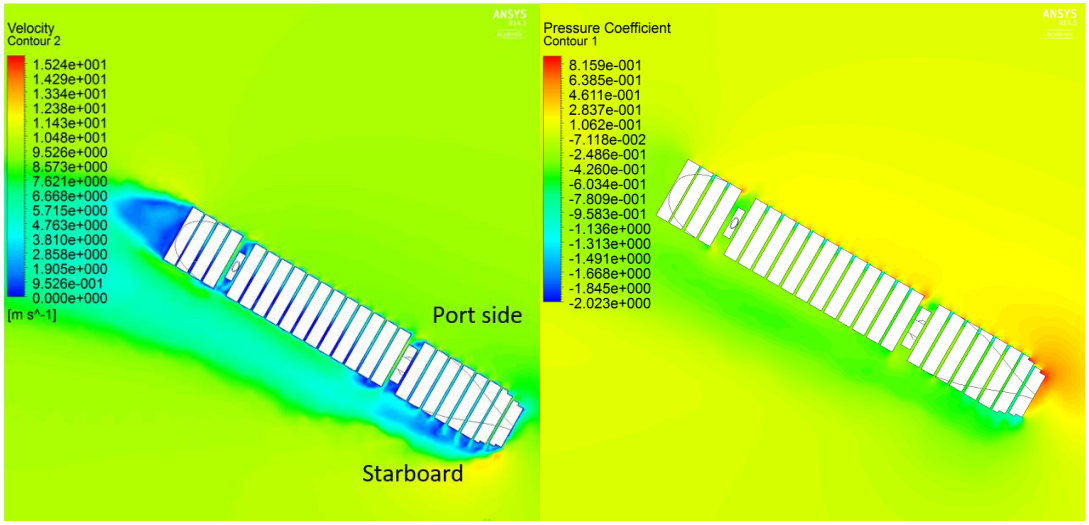

Figure 9: Velocity and distribution of standard model at z=0.12m

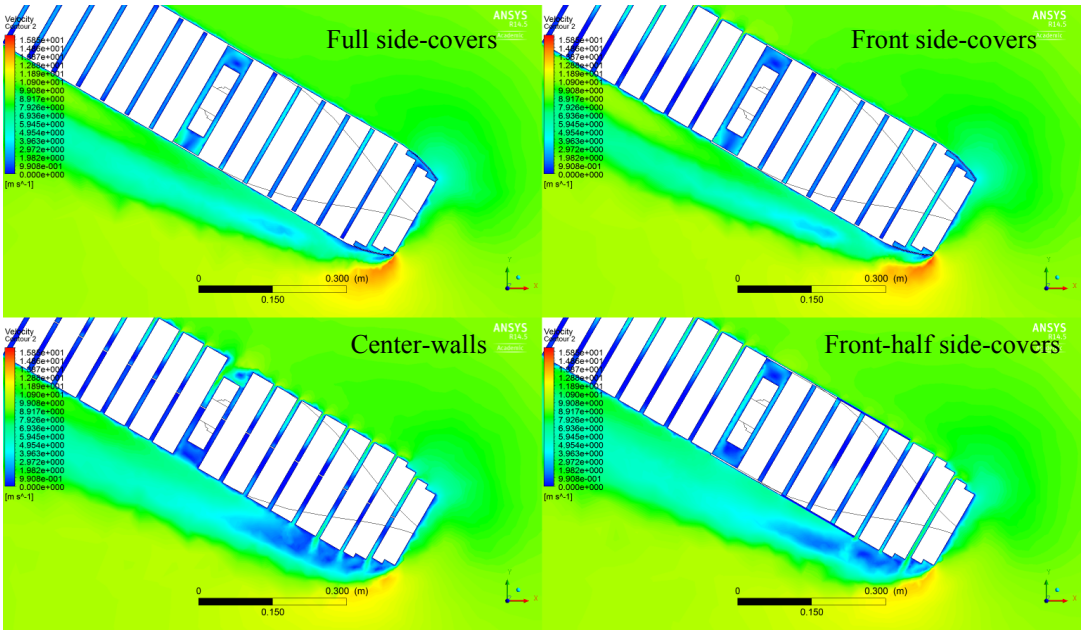

Figure 10: Velocity distribution at z=0.12m

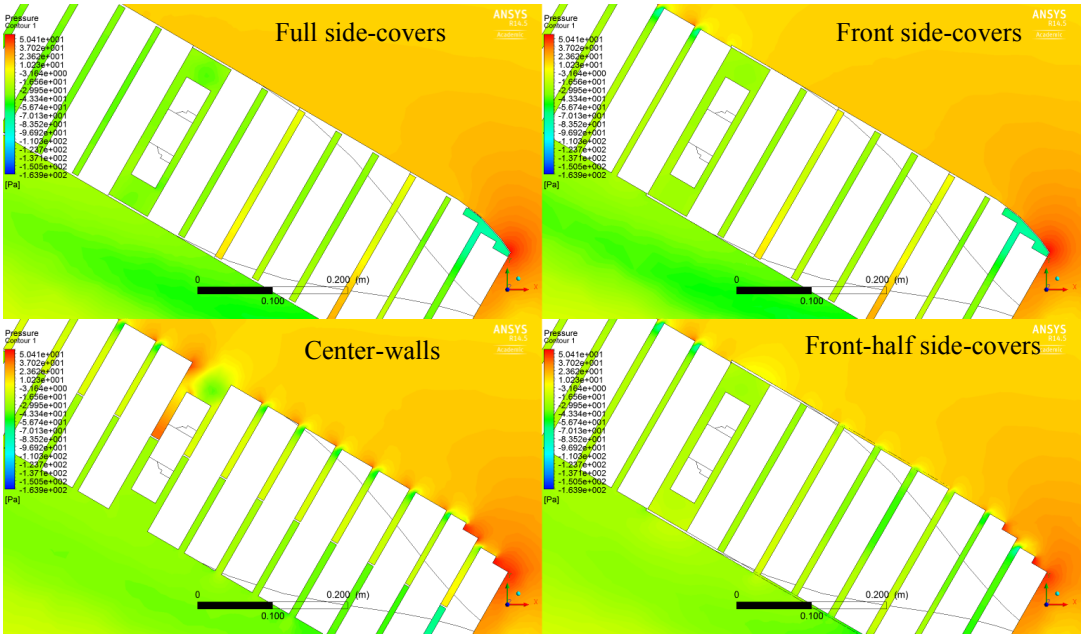

Figure 11: Pressure distribution at z=0.12m

5.2 Velocity Vectors and Streamlines

The velocity vectors and streamlines took at/from the horizontal plane z=0.12m are presented in Figs. 12 and 13.

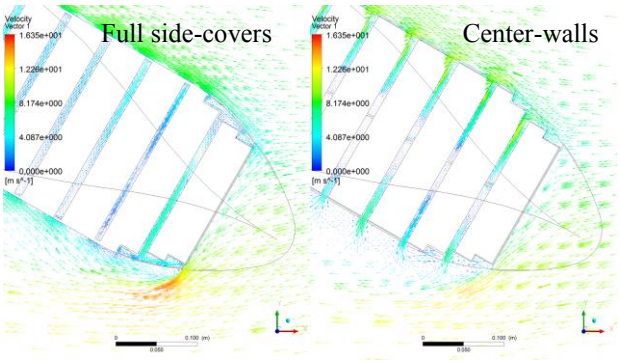

Figure 12: Velocity vectors at z=0.12m

Fig. 12 shows that the side-covers shut the flows that across the gaps between deck containers, while the center walls only stop the flows across the center. Nevertheless, the flows can enter or escape the gap from each side. That is the reason why the wake appears on the starboard side of the center walls model.

Fig. 13 show that the full side-covers and the front side-covers reduce the vortex generated at the starboard side, while the front-half side-covers and center-wall models have large wakes at the bow starboard side.

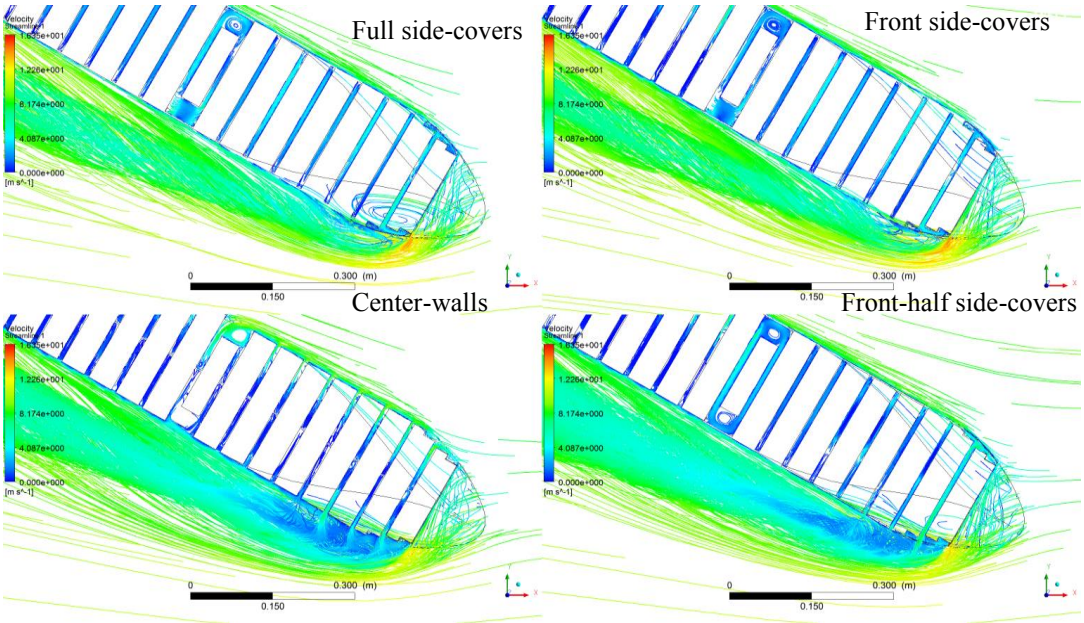

Figure 13: Streamlines distribution from z=0.12m

5.3 Aerodynamic Coefficients

In the previous study [4] it has been confirmed that the air resistance in headwinds can be reduced by up to 20% by using apparatuses. The target of the present study is to reduce the air resistance in oblique winds.

The aerodynamic coefficients of the container ship models at wind angle from 0 to 180 degrees are presented in Figs. 14 ~ 16. It should be noted that in the figures the calculated ones up to 30 degrees of wind angle are shown for the cases of the front side-covers and the front-half side-covers.

Fig. 14 shows that at 30 degrees, the maximum reduction of the air resistance, more than 50%, is obtained by the full side-covers, and the front side-covers follow it. The front-half side-covers and the center-walls are not so effective. The reason can be understood from the pressure distribution shown in Fig. 11. The full side-covers shut all the gap flows, then the pressures acting on the frontal side and the back side of each container on deck are almost same. This means that no added air resistance is generated by the gaps.

The results demonstrate that at 60 degrees of wind angle, the full side-covers produce the thrust although the resistances are created for other cases.

In the following wind, the full side-covers generate much smaller thrust than the center walls and standard models.

Figs. 15 and 16 show that the side-covers increases the side force at the wind angle from 60 to 150 degrees, and increases the yaw moment from 30 to 60 degrees and 120 to 150 degrees.

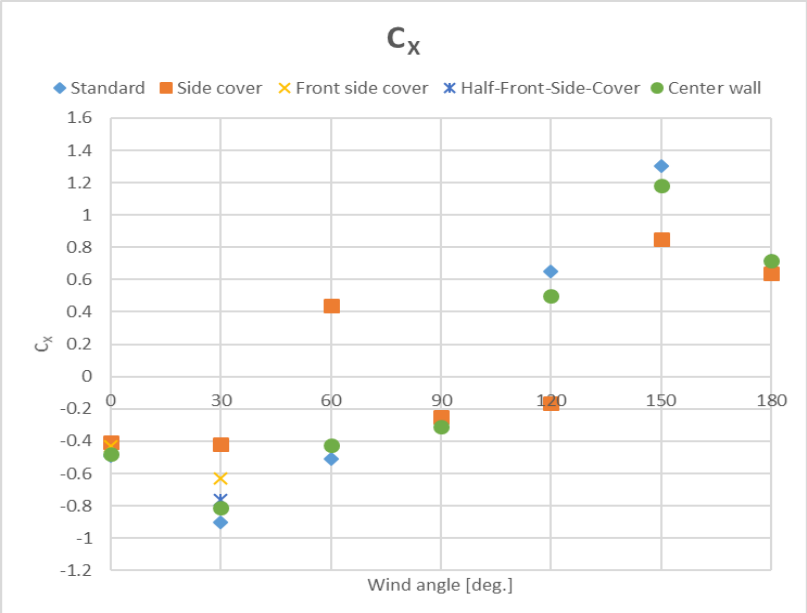

Figure 14: Longitudinal force coefficients

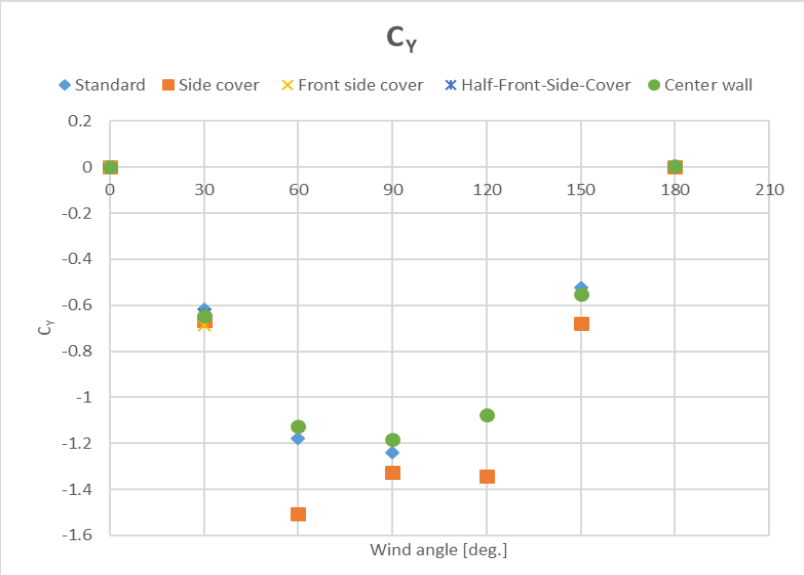

Figure 15: Side force coefficients

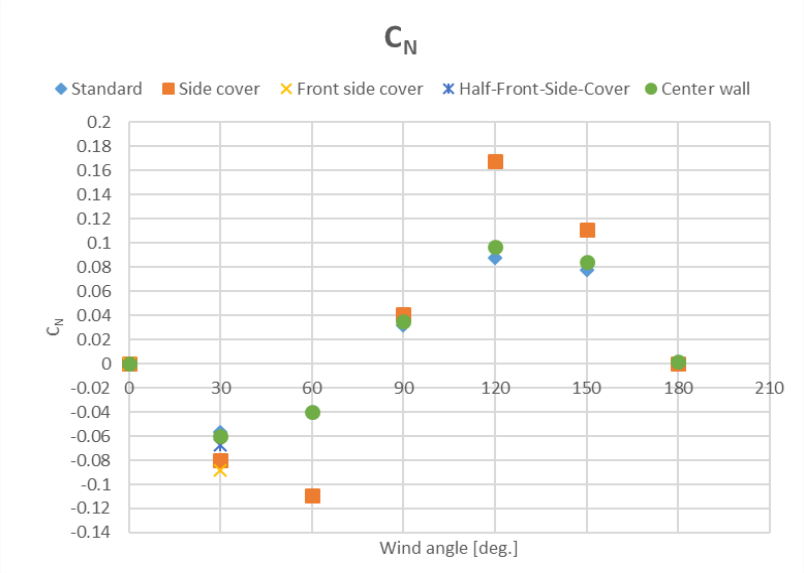

Figure 16: Yaw moment coefficients

The longitudinal force coefficients, or the resistance coefficient, and its reduction at the wind angle of 0 and 30degrees are summarized in Table 3. The results in the table show that in a headwind, the side-covers can reduce the air resistance by up to 10~18%. While the center-walls only reduces the air resistance by only about 3%. At 30 degrees of wind angle, the reduction of air resistance is proportional to the size of side covers. They are 50%, 30%, and 15% for the full side covers, front side covers and front-half side covers, respectively. The center-walls shows only 10% reduction.

Table 3: Longitudinal force coefficient and its reduction at 0 and 30degrees of wind angles

0degree	**Cx**	**ΔCx (%)**
Standard	-0.4926	-
Full side covers	-0.4063	-17.52
Front side covers	-0.4326	-12.19
Front-half side covers	-0.4458	-9.50
Center walls	-0.4809	-2.37
30degrees	**Cx**	**Δ Cx (%)**
Standard	-0.9012	-
Full side covers	-0.4204	-53.35
Front side covers	-0.6313	-29.94
Front-half side covers	-0.7619	-15.45
Center walls	-0.8100	-10.12

6 CONCLUSIONS

- The aerodynamic forces acting on a 20000TEU container ship model in the fully loaded deck-containers condition in oblique winds are numerically investigated by using a commercial CFD code.
- The numerical results show that the air resistance is caused by high pressure acting on each corner of the deck container blocks.
- Fully or partially closing the gaps between deck-containers by using side-covers and a center-wall can reduce the air resistance.
- The reduction of air resistance is proportional to the size of side covers.
- The reductions of the air resistance at 30 degrees of wind angle are up to 50%-30%-15%-10% by the full side-covers, front side-covers, front-half side-covers, and the center-wall, respectively.

REFERENCES

[1] K. Ouchi, Y. Tanaka, A. Taniguchi, J. Takashina, N. Matsubara, and K. Kimura, "A study on air drag reduction on the large container ship in the sea," in *Proc. of Int. conf. Design & Operation of Container Ships*, 2014, no. May, pp. 107–114.

[2] Y. Kim, K. Kim, S. Jeong, S. Jeong, S. Van, Y.-C. Kim, and J. Kim, "Design and Performance Evaluation of Superstructure Modification for Air Drag Reduction of a Container Ship," in *Proc. 25th Int. Ocean and Polar Engineering Conf.*, 2015, no. February 2015, pp. 894–901.

[3] I. Watanabe, V. T. Nguyen, S. Miyake, N. Shimizu, and Y. Ikeda, "A Study on Reduction of Air Resistance acting on a Large Container Ship," in *Proc. of APHydro2016*, 2016, pp. 321–330.

[4] V. T. Nguyen, A. Kinugawa, N. Shimizu, and Y. Ikeda, "Studies on Air Resistance Reduction Methods for a Large Container Ship (Part 1)," in *Proc. JASNAOE Annual Autumn Meeting*, 2016, pp. 427–432.